



Benham, A.M., Van Lith, M., Sitia, R., and Braakman, I. (2013) Ero1-PDI interactions, the response to redox flux and the implications for disulfide bond formation in the mammalian endoplasmic reticulum. *Philosophical Transactions of the Royal Society of London Series B: Biological Sciences*, 368 (1617). Art. 20110403. ISSN 0962-8436

Copyright © 2013 The Authors

<http://eprints.gla.ac.uk/79062/>

Deposited on: 7 May 2013



**Cite this article:** Benham AM, van Lith M, Sitia R, Braakman I. 2013 Ero1–PDI interactions, the response to redox flux and the implications for disulfide bond formation in the mammalian endoplasmic reticulum. *Phil Trans R Soc B* 368: 20110403.

<http://dx.doi.org/10.1098/rstb.2011.0403>

One contribution of 11 to a Theme Issue 'Assemble chaperones in health and disease'.

**Subject Areas:**

biochemistry, cellular biology

**Keywords:**

chaperone, endoplasmic reticulum, protein folding, redox, disulfide bond

**Author for correspondence:**

Adam M. Benham

e-mail: [adam.benham@durham.ac.uk](mailto:adam.benham@durham.ac.uk)

# Ero1–PDI interactions, the response to redox flux and the implications for disulfide bond formation in the mammalian endoplasmic reticulum

Adam M. Benham<sup>1</sup>, Marcel van Lith<sup>1,2</sup>, Roberto Sitia<sup>3,4</sup> and Ineke Braakman<sup>5</sup>

<sup>1</sup>School of Biological and Biomedical Sciences, Durham University, South Road, Durham DH1 3LE, UK

<sup>2</sup>College of Medical, Veterinary and Life Sciences, Davidson Building, University of Glasgow, Glasgow G12 8QQ, UK

<sup>3</sup>Università Vita-Salute San Raffaele, DiBiT, Via Olgettina 58, 20132 Milano, Italy

<sup>4</sup>Division of Genetics and Cell Biology, San Raffaele Scientific Institute (OSR), Milan, Italy

<sup>5</sup>Cellular Protein Chemistry, Faculty of Science, Utrecht University, Padualaan 8, 3584 Utrecht, The Netherlands

The protein folding machinery of the endoplasmic reticulum (ER) ensures that proteins entering the eukaryotic secretory pathway acquire appropriate post-translational modifications and reach a stably folded state. An important component of this protein folding process is the supply of disulfide bonds. These are introduced into client proteins by ER resident oxidoreductases, including ER oxidoreductin 1 (Ero1). Ero1 is usually considered to function in a linear pathway, by 'donating' a disulfide bond to protein disulfide isomerase (PDI) and receiving electrons that are passed on to the terminal electron acceptor molecular oxygen. PDI engages with a range of clients as the direct catalyst of disulfide bond formation, isomerization or reduction. In this paper, we will consider the interactions of Ero1 with PDI family proteins and chaperones, highlighting the effect that redox flux has on Ero1 partnerships. In addition, we will discuss whether higher order protein complexes play a role in Ero1 function.

## 1. Oxidative protein folding in the endoplasmic reticulum

Disulfide bonds are formed between two cysteine residues, either within proteins (intramolecular disulfides) or between proteins (intermolecular disulfides) [1]. This is a rare occurrence in the cell cytosol because the reducing environment favours free thiols (–SH). However, in the bacterial periplasm [2], the mitochondrial intermembrane space and the eukaryotic endoplasmic reticulum (ER [3]), the environment is more oxidizing and favours disulfide bond formation (S–S). In the ER, native disulfide bonds are integrated into proteins early during the folding process [4]. This occurs while the protein is being threaded through the translocon during, or shortly after, translation. The process of ensuring that a protein is properly folded and equipped with the correct disulfide bond arrangements is carefully coordinated by various protein disulfide isomerases (PDIs), oxidoreductases, chaperones and other folding factors [5]. These folding assistants ensure that disulfide bond formation is coupled to other post-translational modifications, such as the introduction of N-linked glycans and to quality control processes [6]. The main players involved in oxidative folding and quality control have been identified, but how they interact and work together in a coordinated fashion is not fully understood. The ER can be viewed as the control point for a cell's secretory output and for the integrity of proteins within the secretory pathway itself. Thus, understanding how the ER machinery works in different cells and tissues is essential for us to tackle various biological problems, ranging from diseases of misfolding to the need for improved production of recombinant proteins.

## 2. Protein disulfide isomerase and Ero1

Two of the major contributors to disulfide bond formation in the ER are PDI and the ER oxidoreductin (or oxidoreductase) Ero1. There is a solitary Ero1 protein in *Saccharomyces cerevisiae* (Ero1p [7,8]) and two (Ero1 $\alpha$  and Ero1 $\beta$  [9,10]) in mammals. Together, PDI and Ero1 proteins harness the oxidizing power of molecular oxygen to create de novo disulfide bonds in a newly folding protein [11,12]. The exchange of disulfide bonds from Ero1 to PDI to client necessitates electron flow in the reverse direction, from client to PDI to Ero1. Ero1s use the cofactor flavin adenine dinucleotide (FAD) to reduce molecular oxygen, generating peroxide in the process [13,14]. PDI is able to supply, rearrange (isomerize) or reduce disulfide bonds in a client protein [15]. The ability of PDI to perform these functions depends on its two redox-active **a** and **a'** thioredoxin domains [16]. The **a** type domains are separated by two redox-inactive **b** domains in an **abb'xa'** arrangement [17,18], where the **x** linker region contributes to mobility and modulates client access to PDI [19,20]. The PDI **a** type domains have CGHC active sites: their high biochemical reduction potential ( $-180$  mV) makes PDI thermodynamically suited for donating disulfide bonds to reduced protein clients [21]. During disulfide bond formation in mammalian cells, the **a** domain of PDI is oxidized by its **a'** domain [22] after the **a'** domain of PDI has been preferentially oxidized by Ero1 $\alpha$  [23,24]. The  $C_{94}xxxxC_{99}$  region ( $x = \text{any amino acid}$ ), on a flexible loop of Ero1 $\alpha$ , effects the transfer of disulfide bonds from Ero1 $\alpha$  to the **a'** domain of PDI [25]. In turn, the  $C_{94}xxxxC_{99}$  site of Ero1 $\alpha$  receives a disulfide bond from the  $C_{394}xxC_{397}$  site, which is in direct communication with the FAD moiety [26]. A similar mechanism occurs in *S. cerevisiae* [27]; however, in yeast, Pdi1p is glycosylated, and in the context of the full-length protein, the **a** domain functions better as an isomerase, with the **a'** domain being a better oxidase [28].

Although Ero1p is essential for yeast (and *Caenorhabditis elegans*) viability, mice deficient in both Ero1 $\alpha$  and Ero1 $\beta$  are viable [29], which stimulated the search for supplementary pathways of disulfide bond formation in the ER (reviewed in [30,31]). Alongside Ero1, additional sources of disulfide bond equivalents to PDI include peroxiredoxin IV [32,33], glutathione peroxidases [34] and vitamin K epoxide reductase [35]. The sulfhydryl oxidase QSOX can oxidize some substrates of the secretory pathway and extracellular matrix directly [36] and the selenoprotein Sep15 may also contribute to disulfide bond reduction/isomerization during glycoprotein quality control [37]. Low molecular weight thiols, principally glutathione, also regulate the redox balance of the ER [38,39].

## 3. The regulatory poise of Ero1 $\alpha$ differs between cell types

Although the general flow of disulfides between Ero1 and PDI is now understood, many key points remain unknown. In higher eukaryotes, there are over 20 PDI homologues. Although some of them lack redox-active **a**-type domains, the majority are likely to be directly involved in disulfide bond formation or regulation [15,40]. In yeast, there is a hierarchy of interactions between Ero1p and the Pdi1p homologues [41], but it is not clear how many PDIs require Ero1 for the provision of disulfide bond equivalents in mammalian cells. Mammalian disulfide bond formation may also be

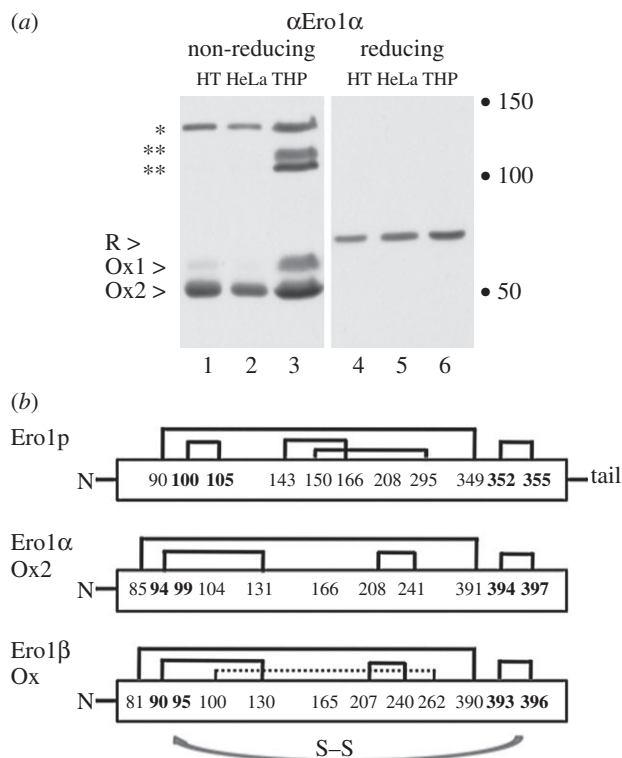


**Figure 1.** The redox state and interactions of Ero1 $\alpha$  are cell-type dependent. (a) Equal amounts of lysates from HT1080 cells (lanes 1 and 4), HeLa cells (lanes 2 and 5) and THP1 cells (lanes 3 and 6) were analysed by non-reducing (lanes 1–3) or reducing (lanes 4–6) SDS-PAGE and probed for Ero1 $\alpha$  expression. Endogenous disulfide-bonded complexes with PDI (asterisk) and other proteins (double asterisk) can be detected at steady state. Molecular weight markers of 50, 100 and 150 kDa are shown as dots. (b) A schematic of the disulfide bonds (black lines) of Ero1p, Ero1 $\alpha$  (Ox2) and Ero1 $\beta$  (Ox). In Ero1 $\alpha$  Ox2, the C94–C131 disulfide precludes formation of a disulfide at the active site C94–C99 (shown in bold). An analogous regulatory disulfide between C90 and C130 is found in Ero1 $\beta$  together with a likely additional long-range disulfide between C100 and C262 (hatched line). Note that the regulatory cysteines differ between Ero1 $\alpha$ / $\beta$  and Ero1p. The most N-terminal cysteine residues are not shown for simplicity. Disulfide bond flow from the C-terminal active site cysteines to the N-terminal active site cysteines (shown in bold) is depicted by a grey arrow.

regulated differently in diverse tissue types or physiological settings. To illustrate this, figure 1 shows an experiment in which the expression of Ero1 $\alpha$  was analysed by Western blotting at steady state in three different cell lines, HT1080 (a fibrosarcoma), HeLa (a cervical carcinoma) and THP1 (a monocytic leukaemia). The proteins in the cell lysates were separated electrophoretically under non-reducing conditions (figure 1a, lanes 1–3), which allow disulfide-dependent interactions to be preserved, and reducing conditions, which instead disrupt disulfide bonds (figure 1a, lanes 4–6). It is known from previously published experiments that under non-reducing conditions, monomeric Ero1 $\alpha$  can exist as a reduced form (R) and two partially oxidized forms, Ox1 and Ox2 [42]. The Ox2 form has a regulatory disulfide bond between C94 and C131 that inactivates the redox activity of Ero1 $\alpha$  [23,43].

Endogenous Ero1 $\alpha$  in HT1080 and HeLa cells was almost exclusively found in the compact Ox2 form (figure 1a, lanes 1 and 2) and represents an inactive reservoir of the protein. By contrast, THP1 cells expressed more of the active Ox1 form of Ero1 $\alpha$  (figure 1a, lane 3). The fully reduced form of Ero1 $\alpha$  was not detectable in either cell line at steady state by the 2G4 antibody. These cell lines do have a high secretory

output, so why should they have a different Ero1 $\alpha$  Ox1 : Ox2 balance? One possibility is that Ero1 $\alpha$  is involved in a wider range of biological processes in monocytes and macrophages, which are professional antigen-presenting cells of the immune system. In support of this idea, it has been shown that Ero1 $\alpha$  regulates the ER calcium channel IP3R and hence indirectly controls the release of calcium from the ER [44], a process that can induce apoptosis [45]. Ero1 $\alpha$  localizes to mitochondrial-associated membranes (MAMs) under oxidizing conditions, where transfer of calcium can occur [44,46,47] and calcium sensing studies using fluorescent probes suggest that calcium levels respond to changes in Ero1 $\alpha$  activity [48]. In cultured macrophages, Ero1 $\alpha$  can subsequently induce the activation of the NADPH oxidase complex [49], which generates superoxide for the destruction of ingested pathogenic bacteria and mycobacteria. NADPH oxidase 2 function is important because genetic defects in components of the complex can lead to X-linked chronic granulomatous disease, which results in life-threatening bacterial infections [50]. It will be interesting to test whether NADPH oxidase activity can be controlled by modulating the Ero1 $\alpha$  oxidation state, and to assess the relative contribution of Ero1 $\alpha$  to calcium signalling compared with oxidative protein folding. Thus, it is becoming apparent that Ero1 $\alpha$  function is not strictly limited to oxidative protein folding, but can contribute to multiple biochemical pathways, including cross-compartmental calcium fluxes and redox communication.

#### 4. Ero1 $\alpha$ engages in multiple disulfide-dependent interactions

Another possible explanation for cell-specific differences in Ero1 $\alpha$  oxidation state is that Ero1 $\alpha$  could be regulated by different PDI family members, such as ERp44, ERp57 and ERp72 [51–54], and these proteins may vary in their ability to reduce Ero1 regulatory disulfide bonds. In support of this idea, the experiment shown in figure 1*a* illustrates that Ero1 $\alpha$  can be trapped in inter-molecular, disulfide-dependent complexes with different partners that vary depending on the cell type. Whereas Ero1 $\alpha$  interacted equally well with a protein that is likely to be PDI (figure 1*a*, asterisk) in all three cell lines, additional inter-molecular Ero1 $\alpha$  interactions can be seen in THP1 cells (figure 1*a*, lane 3, double asterisk). These interacting proteins have yet to be formally identified, but based on published and unpublished data, one is likely to be the PDI homologue ERp44, which was identified as a novel protein important for ER retention of Ero1 $\alpha$  by the Sitia group [51]. ERp44 was subsequently shown to be involved in the quality control of the IgM immunoglobulin [55], adiponectin [56] and the serotonin receptor SERT [57]. These studies suggest that ERp44 is important for the assembly of proteins into oligomers, and probably acts as a platform upon which its clients are assembled prior to delivery to ER exit sites and post-ER compartments such as the ERGIC [58,59]. ERp44 is also important for the regulation of IP3R1 [60], which is of particular interest given the link between Ero1 $\alpha$  and IP3R1 in macrophages discussed in the previous section. ERp44 mutants that bind Ero1 $\alpha$  at high affinity inhibit oxygen consumption [25], but further work is required to determine how ERp44 directly regulates the oxidation state, and hence activity, of Ero1 $\alpha$  in different cell types. However, experiments in transfected HeLa cells have

shown that the interaction between ERp44 and Ero1 $\alpha$  is independent of a hydrophobic hairpin in Ero1 $\alpha$  that is required for full binding of Ero1 $\alpha$  to PDI. PDI and ERp44, therefore, interact with Ero1 $\alpha$  differently, providing scope for fine-tuning the activity of Ero1 $\alpha$  in different cells and tissues [25].

#### 5. Redox-sensitive regulation of Ero1 $\alpha$

Elegant studies with yeast Ero1p [61–63], mammalian Ero1 $\alpha$  [23,24,43,64] and mammalian Ero1 $\beta$  [65] have mapped out the regulatory disulfide bonds that control the activity of Ero1 proteins. These regulatory disulfides and their relationship to the redox-active cysteines are outlined in figure 1*b*. The C94–C131 regulatory disulfide bond in Ero1 $\alpha$  ‘locks down’ residue C94; this prevents the active site C94–C99 disulfide from forming and subsequently donating a disulfide to PDI. The robustness of this intrinsic control system and its very rapid responsiveness to fluctuations in the redox environment is highlighted by three previously unpublished experiments from our laboratories (figures 2–4). HeLa cells transfected with Ero1 $\alpha$  were exposed to various concentrations of the reducing agent dithiothreitol (DTT) in culture, radiolabelled and the DTT quenched with excess *N*-ethylmaleimide (NEM; figure 2). Analysis of the cell lysates by immunoprecipitation and non-reducing sodium dodecyl sulfate–polyacrylamide gel electrophoresis (SDS–PAGE) showed that the inactive oxidized Ox2 form of Ero1 $\alpha$  was readily reduced when 1.25 mM DTT was added to the cell, whereas the partially oxidized (active) Ox1 form could resist reduction, with up to at least 20 mM DTT. Interestingly, a number of additional Ero1 $\alpha$  disulfide-dependent complexes were revealed upon addition of 1.25 mM DTT (figure 2*a*, lane 2). These complexes may represent oligomers that reside in higher molecular-weight complexes during oxidizing conditions. The Ero1 $\alpha$  associated proteins may be additional regulatory or accessory proteins (such as chaperones or PDI family members) that are recruited to Ox1 or to partially reduced Ero1 $\alpha$  during the oxidation cycle. The bands in the 75–150 kDa region of the gel are likely to represent specific disulfide-dependent protein interactions with Ero1 $\alpha$  because they are reduced by adding DTT to the sample buffer prior to SDS–PAGE (figure 2*b*).

As the DTT concentration applied to the living cell was increased, the intensity of the Ox2 signal declined (figure 2*a*, lanes 1–2), as did the total Ero1 $\alpha$  signal (figure 2*b*, lanes 1–2). Because the signal of PDI (immunoprecipitated from the same lysates) remained similar between 0 and 1.25 mM DTT (figure 2*c*, lanes 1–2), the loss of signal was Ero1 $\alpha$  specific. The loss of signal could reflect impaired detergent solubility in Triton X-100 owing to aggregation, loss of protein owing to degradation by ER quality control mechanisms or loss of antibody reactivity after post-translational modification. However, given the fact that the polyclonal antiserum recognizes a range of conformations and redox states of Ero1 $\alpha$ , we favour the former explanation. Given the relationship between Ero1 $\alpha$  and calcium signalling described above, it would be intriguing to determine whether the changes in Ero1 $\alpha$  signal intensity relate to its recruitment to MAMs or to ER detergent-resistant membranes in a redox-dependent manner.

The DTT-induced change from Ox2 to Ox1 can be explained structurally by the transition of Ero1 $\alpha$  from a compact form with an intact regulatory C94–C131 disulfide (Ox2) to a more ‘open’ active form (Ox1) in which the regulatory

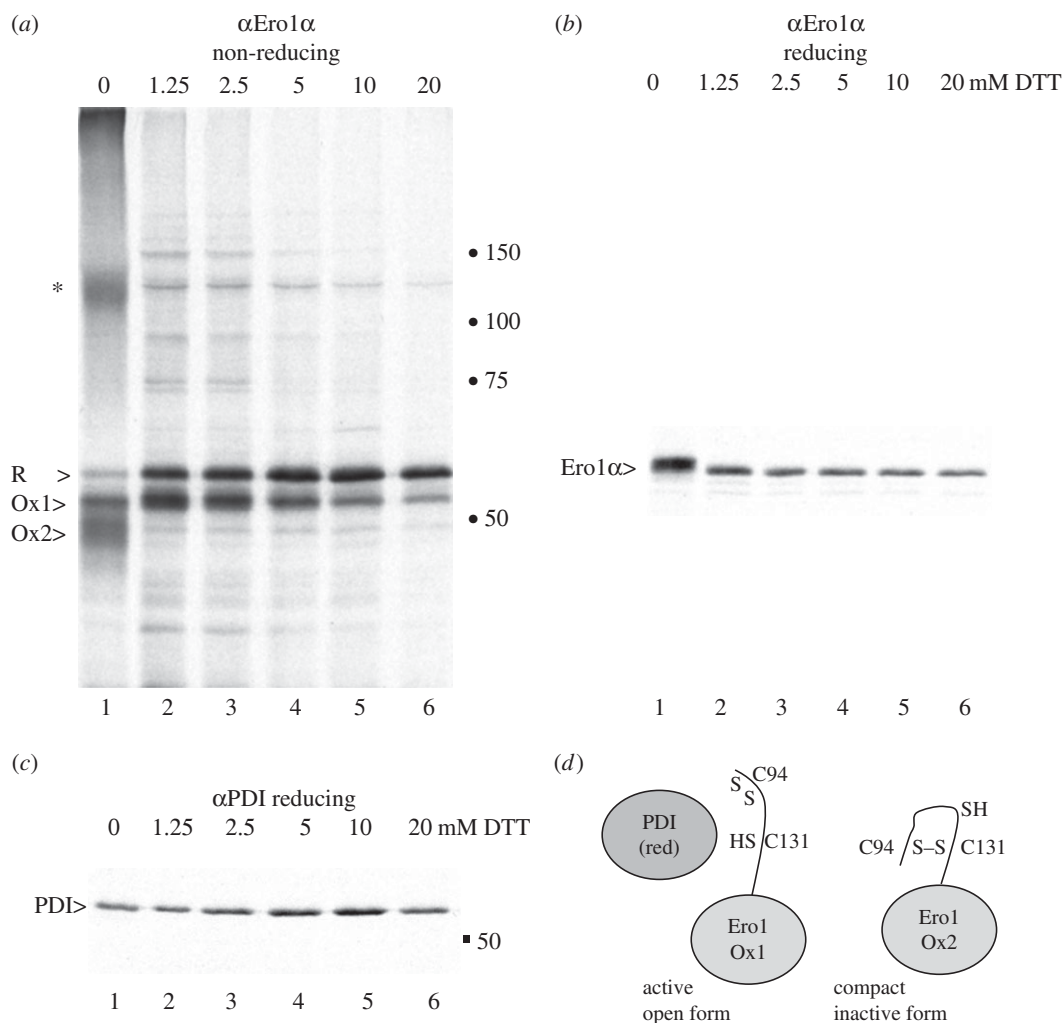


**Figure 2.** Selective reduction of Ero1 $\alpha$  complexes. HeLa cells transfected with Ero1 $\alpha$  were metabolically labelled for 5 min in the presence of 0, 1.25, 2.5, 5, 10 or 20 mM DTT and post-nuclear lysates subjected to immunoprecipitation using antibody D5. Samples were analysed on (a) non-reducing or (b) reducing 7.5% SDS-PAGE. The 120 kDa complex is indicated by an asterisk and molecular weight markers of 50, 75, 100 and 150 kDa are shown as dots. Alternatively,  $\alpha$ PDI was used to retrieve PDI from the same lysates prior to analysis on reducing 7.5% SDS-PAGE (c). Ero1 $\alpha$  R, Ox1 and Ox2 are indicated by greater than symbol (>). (d) Cartoon to illustrate the active 'open' form of Ero1 $\alpha$  Ox1 compared with the more compact Ero1 $\alpha$  Ox2. Ox1 lacks the regulatory C94–C131 disulfide and recruits reduced PDI for re-oxidation. For simplicity, only C94–C99 is shown. The higher apparent molecular weight of Ero1 $\alpha$  in (b) lane 1 could be due to increased binding of NEM to more free cysteines, a change in the accessibility of a cysteine residue(s) to NEM or an alternative, redox-dependent post-translational modification at a cysteine residue.

disulfide has been broken by DTT (figure 2d). The Ero1 $\alpha$  C94–C99 disulfide is consequently primed to donate a disulfide to reduced PDI, which lacks regulatory disulfides.

## 6. Dithiothreitol-induced structural changes in Ero1 $\alpha$ are reversible

To respond to changes in the redox environment, Ero1 $\alpha$  must switch rapidly between active and inactive states. To assess how rapidly Ero1 $\alpha$  altered its equilibrium when exposed to a redox shift, we investigated how the protein responded when oxidizing conditions were restored after a 5 min challenge with 5 mM DTT (figure 3). Ero1 $\alpha$  partitions into R and active Ox1 during the 5 min pulse, with the Ero1 $\alpha$ –PDI complex maintained under these conditions (figure 3a, lane 1). From previously published work, the Ero1 $\alpha$ –PDI complex is likely to comprise both mature and radiolabelled PDI and Ero1 $\alpha$  [42]. When DTT was washed out, the normal oxidation pattern of Ero1 $\alpha$  was restored within 10 mins. The diffuse 120 kDa complex (\*) and higher molecular weight

complexes reformed within 3 min (figure 3a, lane 2). Re-oxidation of Ero1 $\alpha$  resulted in rapid recovery of the inactive Ox2 form demonstrating that Ero1 $\alpha$  is responsive to changes in the ER redox state.

Observation of the reducing gel showed an increase in the total Ero1 $\alpha$  signal retrieved when cells were shifted from reducing to oxidizing conditions (figure 3a, lanes 5 and 6). Consistent with this experiment, the opposite pattern was seen when cells were shifted from oxidizing to reducing conditions (figure 2b, lanes 1 and 2). This observation shows that the decrease in signal in figure 2b cannot be explained by degradation of Ero1 $\alpha$ . Ero1 $\alpha$  became more accessible to NEM when the reducing agent was removed and the environment was made more oxidizing (compare figure 3a, lanes 5 and 6 with figure 2b, lanes 1–2), consistent with the finding that Ero1 $\beta$  FAD-binding site mutants make cysteines available in a temperature- or stress-dependent manner [66]. This somewhat counterintuitive finding is illustrated schematically in figure 3b. When Ero1 $\alpha$  is covalently modified by NEM, it gains molecular weight and hence runs more slowly (higher up) in a reducing gel. Ero1 $\alpha$  in the Ox2 form

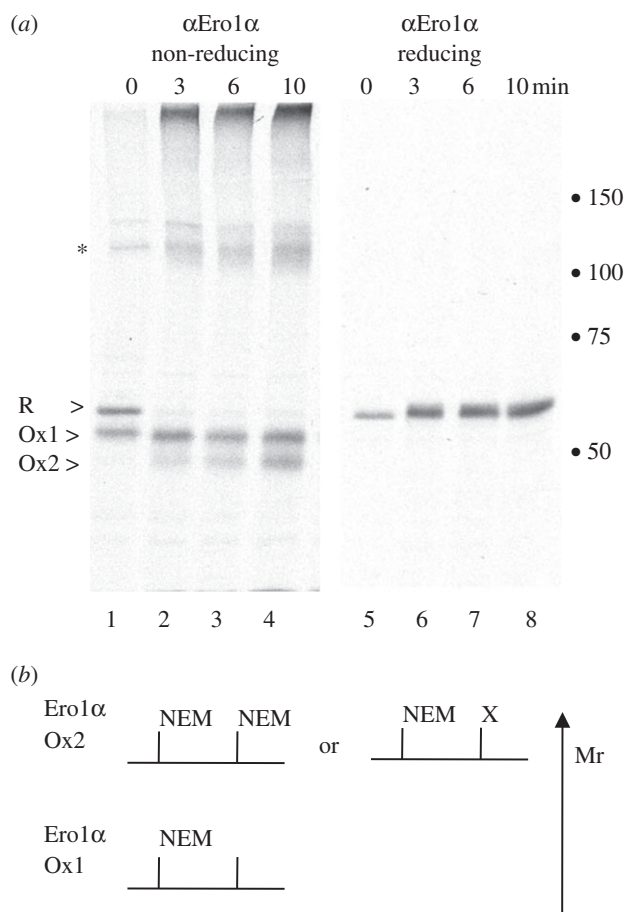


**Figure 3.** Post-translational oxidation of Ero1 $\alpha$ . (a) HeLa cells transfected with pcDNA3.1-Ero1 $\alpha$  were metabolically labelled for 5 min in the presence of 5 mM DTT and then chased for 0, 3, 6 or 10 min. Cell lysates were subjected to immunoprecipitation with D5 and analysed on non-reducing (lanes 1–4) or reducing (lanes 5–8) 7.5% SDS-PAGE. The Ero1 $\alpha$  forms R, Ox1, Ox2 and the 120 kDa complex (asterisk) are shown. Dots represent 50, 75, 100 and 150 kDa markers. (b) Schematic to explain the mobility shift of Ero1 $\alpha$  when analysed by reducing SDS-PAGE. After removal of DTT, Ox2 (and Ero1 $\alpha$ -associated complexes) reappear and are more readily alkylated by NEM, increasing the molecular weight (Mr). X represents putative post-translational modifications that could also increase Ero1 $\alpha$  molecular weight.

and/or Ero1 $\alpha$  in higher molecular weight complexes must have either (i) more free cysteine residues than partially reduced Ero1 $\alpha$ , (ii) cysteine residues that are less buried and hence more accessible to NEM, or (iii) cysteine residues that are subject to alternative post-translational modifications under oxidizing conditions, such as glutathionylation at an unpaired cysteine.

## 7. Ero1 $\alpha$ interactions are differentially sensitive to oxidation cycles within the endoplasmic reticulum

The experiment in figure 3 shows how the Ero1 $\alpha$  intramolecular redox switch can counterbalance changes in the ER redox state within minutes. Having shown that a reducing ER could alter the monomeric and oligomeric equilibrium of Ero1 $\alpha$ , we investigated how Ero1 $\alpha$  would respond when the ER was made more oxidizing. For this, we used the cell-permeable oxidant diamide, which can alter the redox

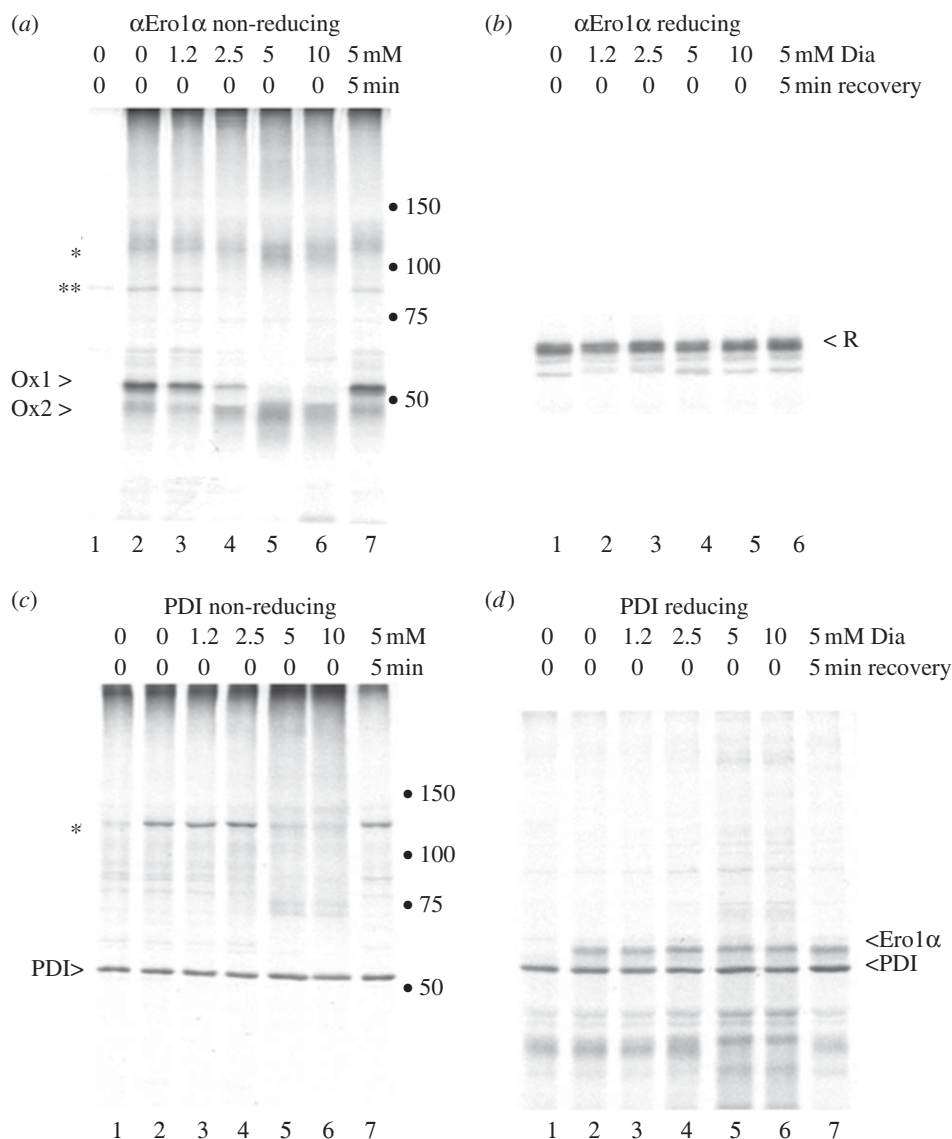
potential of the cell by oxidizing glutathione [67]. Because diamide can decrease the amount of radiolabelling when added during the pulse, Ero1 $\alpha$ -transfected HeLa cells were pulsed in the presence of DTT and then chased in the presence of diamide. These conditions allowed us to follow the fate of a synchronized Ero1 $\alpha$  population and its response to an oxidative flux. Ero1 $\alpha$  and PDI were immunoprecipitated from transfected HeLa cell lysates as before, prior to analysis on 7.5 per cent SDS-PAGE.

Figure 4 shows the result from such an experiment. Ero1 $\alpha$  immunoprecipitations from mock-transfected cells were clear of signal (figure 4a, lane 1). After a pulse without a diamide chase, Ero1 $\alpha$  existed as Ox1 and Ox2, a smeary 120 kDa form and some higher molecular weight complexes that likely include Ero1 $\alpha$ -ERp44 (double asterisk; figure 4a, lane 2). When the chase was supplemented with increasing concentrations of diamide, Ox1 disappeared at the expense of the more compact Ox2 form (figure 4a, lanes 4–6). When Ero1 $\alpha$  was allowed to recover from the diamide treatment by incubating the cells in normal chase medium, the protein returned to Ox1 (figure 4a, lane 7). The upper part of the non-reducing gels (figure 4a,c, lanes 2–7) showed that the diffuse 120 kDa complex persisted during diamide treatment, but also became more oxidized and compact. The complex returned to its original status when diamide was removed (figure 4a,c, lane 7). The reducing gel shows that in all lanes similar amounts of Ero1 $\alpha$  were recovered when fully reduced in sample buffer (figure 4b, lanes 1–6). This result demonstrated that the various oxidized forms of Ero1 $\alpha$  were not in a simple precursor–product relationship, but were in a dynamic equilibrium with each other that changed according to the redox status of the cell. Re-establishment of the *status quo* occurred within 5 min of removal of the oxidant.

When PDI was immunoprecipitated from the same cell lysates, it formed the expected approximately 120 kDa complex with Ero1 $\alpha$  when visualized under non-reducing conditions (figure 4c, lane 2). Upon reduction, the Ero1 $\alpha$ –PDI complex was disrupted and monomeric Ero1 $\alpha$  was recovered (figure 4d, lane 2). However, when diamide was added at 5 mM or more, the dimeric 120 kDa PDI–Ero1 $\alpha$  complex disappeared (figure 4c, lanes 5–6). Observation of the reducing gels (figure 4d, lanes 5 and 6) revealed that Ero1 $\alpha$  could still be recovered in the PDI immunoprecipitates, indicating that PDI and Ero1 $\alpha$  were interacting in the higher molecular weight disulfide-bonded complexes under these conditions. The 120 kDa PDI–Ero1 $\alpha$  complex rapidly reappeared when diamide was washed out (figure 4c, lane 7).

The loss of the PDI–Ero1 dimer after 5 mM diamide treatment correlates with the loss of Ox1, consistent with the finding that Ox1 is the active form of Ero1 $\alpha$  [43]. However, Ero1 $\alpha$  complexes persisted after 5 and 10 mM diamide treatment (figure 4a, lanes 4–5, asterisk). This smear may include Ero1 $\alpha$  homodimers or other as yet unidentified proteins that interact with and perhaps regulate Ero1 $\alpha$ . The constant Ero1 $\alpha$  signal in the  $\alpha$ PDI immunoprecipitation (figure 4d) also suggests that PDI and Ero1 $\alpha$  may be recruited to larger complexes when the ER becomes more oxidizing.

Strikingly, Ero1 $\alpha$ –PDI dimers and the active Ox1 form of Ero1 $\alpha$  are lost under oxidizing conditions when there is less need for de novo disulfide bond formation. The PDI–Ero1 $\alpha$  pathway for disulfide bond formation is, therefore, sensitive to the redox state of the ER and may recruit different regulators during the redox cycle.



**Figure 4.** The response of Ero1 $\alpha$  to an oxidative wave. HeLa cells transfected with pcDNA3.1-Ero1 $\alpha$  (*a,c* and *d*, lanes 2–7; *b*, lanes 1–6) or mock-transfected cells (*a,c* and *d*, lane 1) were metabolically labelled in the presence of 5 mM DTT and then washed and chased for 10 min in the presence of 0, 1.2, 2.5, 5 and 10 mM diamide (Dia). A 5 mM diamide-treated dish then was allowed to recover by washing and chasing with normal chase medium for 5 min (*a,c* and *d*, lane 7; *b* lane 6). Ero1 $\alpha$  (*a* and *b*) or PDI (*c* and *d*) were immunoprecipitated from the cell lysates and analysed on non-reducing (*a,c*) or reducing (*b,d*) 7.5% SDS-PAGE. Ero1 $\alpha$  R, Ox1 and Ox2, together with the 120 kDa complex (asterisk) and an additional S–S linked complex (double asterisk) are indicated. Dots represent 50, 75, 100 and 150 kDa markers.

## 8. Implications for oxidative protein folding *in vivo*

Ero1 $\alpha$  is an unusual example of a redox-active protein with conformation-dependent, DTT-resistant domains. Experiments from multiple laboratories, including ours, showed that Ero1 is redox regulated (reviewed in [68]). This is reflected in the relative distribution and dynamic response of Ero1 $\alpha$  Ox1 (active) and Ox2 (inactive) to ER redox flux. PDI and Ero1 $\alpha$  participate in a buffered feedback loop that maintains disulfide bond formation at an appropriate level when ER redox conditions fluctuate. Strongly reducing conditions disrupt Ero1 $\beta$ –PDI complexes at steady state [66,69], so it will be informative to directly compare the interactions of glycosylated Ero1 $\alpha$  and Ero1 $\beta$  with PDI. *In vivo*, cells will not encounter DTT or diamide, but will be exposed to a range of physiological redox-active species; so how Ero1 $\alpha$  and PDI respond to reactive oxygen species during hypoxia, nutrient flux and metabolic stress is an important question for the future.

Reduction of the Ero1 regulatory disulfides, by PDI or other mechanisms, is necessary for its activation [68]. Similarly, the redox-dependent Ox1–Ox2 transition from an active to an inactive form is likely to be important in preventing hyper-oxidation, which might be detrimental for reactions requiring PDI-dependent isomerization or reduction of substrates. Active Ox1 is decommissioned when required, supported by our experiments in which Ero1 rapidly and reversibly converts to Ox2 after diamide treatment (figure 4). The very strong inherent redox regulatory capacity of Ero1 $\alpha$  has been confirmed by RNAi knockdown experiments in which the contributions of Ero1 $\alpha$ , peroxiredoxin IV and vitamin K epoxide reductase (VKOR) to oxidative refolding of albumin were compared side by side [70]. Knockdown of Ero1 $\alpha$  gave the most severe delay in recovery of oxidative protein folding, confirming that the Ero1–PDI pathway is the primary source of oxidizing equivalents. Whether this holds for all types of protein clients and all physiological conditions remains to be established.

## 9. Evidence for an oxidative protein folding 'machine' in the endoplasmic reticulum

Experiments presented here and in the literature show that Ero1 $\alpha$  interacts specifically with PDI [42] and ERp44 [51] in disulfide-bonded complexes, and with itself as a homodimer [69]. Here, we show that other interactions are possible under mildly reducing conditions (figure 2). A number of discrete proteins disulfide-linked to Ero1 $\alpha$  appear when the redox balance is altered. Whether these proteins are components of a larger ER-resident machine for the control of oxidative protein folding is open to question. One possibility is that other proteins involved in disulfide bond formation and regulation such as peroxiredoxin IV, glutathione peroxidases and VKOR are brought together with PDI and Ero1 $\alpha$ , perhaps to ER subdomains in a redox-dependent manner. In support of this idea, we note from many of our Ero1 $\alpha$  immunoprecipitation and blotting experiments that complexes resolve towards the top of the stacking gel on non-reducing SDS-PAGE; these complex(es) readily reform when normal conditions are restored after redox flux (e.g. figure 3). Although it is possible that these complexes contain misfolded Ero1 $\alpha$ , the expression levels of Ero1 $\alpha$  in transfection experiments are comparable with endogenous levels of Ero1 in some tissues [29,69] and after induction of Ero1 $\alpha$  by the unfolded protein response or by hypoxia [71,72]. Disulfide trapping combined with SDS-PAGE is an excellent tool for identifying potential redox-active partnerships, but it cannot discriminate between different higher-order complexes that may exist under native conditions. Some attempt has been made to probe the nature of Ero1 complexes *in vivo* using gel filtration. For example, analysis of Ero1 $\beta$  from the stomach and pancreas, where Ero1 $\beta$  is highly expressed, shows that the majority of Ero1 $\beta$  elutes with a profile consistent with that of a complex [69].

Other chaperone networks in the ER have been detected, with BiP (Grp78) a key protein hub for mediating interactions with components of the translocation, protein folding and stress sensing machineries (e.g. [73–75]). By associating with different PDI family members, BiP can be involved in both productive oxidative protein folding (by associating with PDI) and in reductive unfolding for protein degradation (by associating with ERdj5) [76,77]. BiP may be able to multi-task partly because of regulation by post-translational modifications: ADP-ribosylation of BiP has recently been shown to be important for BiP involvement in the unfolded protein response [78]. However, our understanding of the interplay between different ER chaperones remains incomplete. As an example, Jansen *et al.* [79] have proposed an interaction map for ER chaperones that highlights a hitherto unappreciated role of cyclophilins in the function of PDI proteins. Cyclophilin B can interact with at least PDI, ERp72 and P5 and there are additional interactions between ER-localized FK-binding proteins and ERp57, ERp29 and ERp19. It is clear that different protein folding complexes exist in the ER and it will be interesting to see how Ero1 proteins functionally relate to these networks, particularly during times of physiological stress or high secretory demand.

## 10. Material and methods

### (a) Cell lines

The monocytic cell line THP1 (gift from J. Robinson) was maintained in Roswell Park Memorial Institute medium, the fibrosarcoma HT1080 was maintained in Dulbecco's modified Eagle's medium

(DMEM) and the human cervical carcinoma cell line HeLa was maintained in DMEM with non-essential amino acids. The cell lines were supplemented with 8 per cent fetal calf serum (FCS), 100 units ml<sup>-1</sup> penicillin, 100  $\mu$ g ml<sup>-1</sup> streptomycin and 2 mM glutamax and maintained at 37°C and 5 per cent CO<sub>2</sub>.

### (b) Antibodies and cDNA

The polyclonal anti-PDI serum has been described previously [42]. The polyclonal antiserum D5 was raised against non-reduced, reduced and denatured forms of an amylose resin-purified, mannose binding protein–Ero1 $\alpha$  fusion protein (New England Biolabs) expressed in *Escherichia coli* [79]. The monoclonal antibody 2G4 was raised against recombinant full-length Ero1 $\alpha$  [59]. The construction and sequencing of the Ero1 $\alpha$  cDNA behind the T7 promoter in pcDNA3.1 has been previously described [9].

### (c) Transfections

HeLa cells cultured in 6 cm dishes were transiently transfected with 2  $\mu$ g pcDNA3.1-Ero1 $\alpha$  mixed with 10  $\mu$ l lipofectin (Invitrogen) according to the manufacturer's instructions.

### (d) Detection of endogenous Ero1 $\alpha$

HeLa, HT1080 and THP1 cells were lysed in 600  $\mu$ l of lysis buffer (20 mM MES, 30 mM Tris, 100 mM NaCl, pH 7.4), with 1 per cent Triton X-100, 10  $\mu$ g ml each of chymostatin, leupeptin, antipain and pepstatin supplemented with 20 mM NEM as an alkylating agent. Post-nuclear supernatants were prepared by centrifugation at 16 100g for 10 min at 4°C and equal amounts of protein (Bradford assay) were loaded onto SDS-PAGE in Laemmli sample buffer with or without 50 mM DTT as a reducing agent. Proteins were transferred to polyvinylidene difluoride membranes for 2 h and immunodetection was performed using 2G4 Mab tissue culture supernatant as the primary antibody, and 1 : 3000 GAMPO (Dako) as the secondary antibody. Proteins were visualized by enhanced chemiluminescence (GE Healthcare) and exposure to film (Kodak).

### (e) Metabolic labelling and pulse-chase analysis

Sub-confluent HeLa cells in 6 cm dishes were starved with MEM lacking cysteine and methionine (Invitrogen) for 30 min, pulse-labelled for the times stated with 10  $\mu$ Ci [<sup>35</sup>S]-labelling mix per dish and subsequently chased when necessary with complete medium supplemented with 5 per cent FCS, 10 mM HEPES pH 7.4, 5 mM methionine, 5 mM cysteine and 1 mM cycloheximide. At given time intervals, the chase was stopped by flooding the cells with ice-cold HBSS (Invitrogen) supplemented with 20 mM NEM to trap folding intermediates. In some experiments, freshly prepared DTT or diamide (Sigma) solutions were added to the pulse or chase medium, as stated. The cells were lysed in 600  $\mu$ l of lysis buffer (20 mM MES, 30 mM Tris, 100 mM NaCl, pH 7.4), containing 1 per cent Triton X-100, 10  $\mu$ g ml<sup>-1</sup> each of chymostatin, leupeptin, antipain and pepstatin A, 1 mM PMSF, and 20 mM NEM and the nuclei removed by centrifugation for 10 min at 4°C and 16 000 g. Immunoprecipitations were performed at 4°C for either 2 h or overnight using antibodies immobilized on 30  $\mu$ l of a 10 per cent suspension of protein A sepharose beads. Collected complexes were washed twice at room temperature in wash buffer (300 mM NaCl, 0.05% Triton X-100 and 0.05% SDS, 10 mM Tris-HCl, pH 8.6) prior to uptake in sample buffer. After a 3 min incubation at 95°C, half the samples were reduced with 50 mM DTT, and the proteins were analysed by 7.5 per cent SDS-PAGE.

We thank Bertrand Kleizen, Sanjika Dias-Gunasekara and Eelco van Anken for experimental support and numerous members of the A.B., I.B. and R.S. groups for helpful discussions. R.S. was financially supported by Telethon (GGP11077) and Associazione Italiana Ricerca Cancro (IG and 5  $\times$  1000 program). Work in the I.B. laboratory was financially supported by NWO Chemical Sciences and the A.B. laboratory was partly financially supported by the Leverhulme Trust and the Wellcome Trust grant no. 064772.



## References

- Sato Y, Inaba K. 2012 Disulfide bond formation network in the three biological kingdoms, bacteria, fungi and mammals. *FEBS J.* **279**, 2262–2271. (doi:10.1111/j.1742-4658.2012.08593.x)
- Inaba K. 2009 Disulfide bond formation system in *Escherichia coli*. *J. Biochem.* **146**, 591–597. (doi:10.1093/jb/mvp102)
- Riemer J, Bulleid N, Herrmann JM. 2009 Disulfide formation in the ER and mitochondria: two solutions to a common process. *Science* **324**, 1284–1287. (doi:10.1126/science.1170653)
- Braakman I, Bulleid NJ. 2011 Protein folding and modification in the mammalian endoplasmic reticulum. *Annu. Rev. Biochem.* **80**, 71–99. (doi:10.1146/annurev-biochem-062209-093836)
- Feige MJ, Hendershot LM. 2011 Disulfide bonds in ER protein folding and homeostasis. *Curr. Opin. Cell Biol.* **23**, 167–175. (doi:10.1016/j.ceb.2010.10.012)
- Brodsky JL, Skach WR. 2011 Protein folding and quality control in the endoplasmic reticulum: recent lessons from yeast and mammalian cell systems. *Curr. Opin. Cell Biol.* **23**, 464–475. (doi:10.1016/j.ceb.2011.05.004)
- Frand AR, Kaiser CA. 1998 The ER01 gene of yeast is required for oxidation of protein dithiols in the endoplasmic reticulum. *Mol. Cell* **1**, 161–170. (doi:10.1016/S1097-2765(00)80017-9)
- Pollard MG, Travers KJ, Weissman JS. 1998 Ero1p: a novel and ubiquitous protein with an essential role in oxidative protein folding in the endoplasmic reticulum. *Mol. Cell* **1**, 171–182. (doi:10.1016/S1097-2765(00)80018-0)
- Cabibbo A, Pagani M, Fabbri M, Rocchi M, Farmery MR, Bulleid NJ, Sitia R. 2000 ER01-L, a human protein that favors disulfide bond formation in the endoplasmic reticulum. *J. Biol. Chem.* **275**, 4827–4833. (doi:10.1074/jbc.275.7.4827)
- Pagani M *et al.* 2000 Endoplasmic reticulum oxidoreductin 1- $\beta$  (ER01-L $\beta$ ), a human gene induced in the course of the unfolded protein response. *J. Biol. Chem.* **275**, 23 685–23 692. (doi:10.1074/jbc.M003061200)
- Frand AR, Kaiser CA. 1999 Ero1p oxidizes protein disulfide isomerase in a pathway for disulfide bond formation in the endoplasmic reticulum. *Mol. Cell* **4**, 469–477. (doi:10.1016/S1097-2765(00)80198-7)
- Frand AR, Cuozzo JW, Kaiser CA. 2000 Pathways for protein disulphide bond formation. *Trends Cell Biol.* **10**, 203–210. (doi:10.1016/S0962-8924(00)01745-1)
- Tu BP, Weissman JS. 2002 The FAD- and O(2)-dependent reaction cycle of Ero1-mediated oxidative protein folding in the endoplasmic reticulum. *Mol. Cell* **10**, 983–994. (doi:10.1016/S1097-2765(02)00696-2)
- Gross E *et al.* 2006 Generating disulfides enzymatically: reaction products and electron acceptors of the endoplasmic reticulum thiol oxidase Ero1p. *Proc. Natl Acad. Sci. USA* **103**, 299–304. (doi:10.1073/pnas.0506448103)
- Hatahet F, Ruddock LW. 2009 Protein disulfide isomerase: a critical evaluation of its function in disulfide bond formation. *Antioxid. Redox Signal* **11**, 2807–2850. (doi:10.1089/ars.2009.2466)
- Kozlov G, Maattanen P, Thomas DY, Gehring K. 2010 A structural overview of the PDI family of proteins. *FEBS J.* **277**, 3924–3936. (doi:10.1111/j.1742-4658.2010.07793.x)
- Tian G, Xiang S, Noiva R, Lennarz WJ, Schindelin H. 2006 The crystal structure of yeast protein disulfide isomerase suggests cooperativity between its active sites. *Cell* **124**, 61–73. (doi:10.1016/j.cell.2005.10.044)
- Tian G, Kober FX, Lewandrowski U, Sickmann A, Lennarz WJ, Schindelin H. 2008 The catalytic activity of protein-disulfide isomerase requires a conformationally flexible molecule. *J. Biol. Chem.* **283**, 33 630–33 640. (doi:10.1074/jbc.M806026200)
- Nguyen VD *et al.* 2008 Alternative conformations of the x region of human protein disulphide-isomerase modulate exposure of the substrate binding b' domain. *J. Mol. Biol.* **383**, 1144–1155. (doi:10.1016/j.jmb.2008.08.085)
- Wang C *et al.* 2010 Plasticity of human protein disulfide isomerase: evidence for mobility around the X-linker region and its functional significance. *J. Biol. Chem.* **285**, 26 788–26 797. (doi:10.1074/jbc.M110.107839)
- Lundstrom J, Holmgren A. 1993 Determination of the reduction-oxidation potential of the thioredoxin-like domains of protein disulfide-isomerase from the equilibrium with glutathione and thioredoxin. *Biochemistry* **32**, 6649–6655. (doi:10.1021/bi00077a018)
- Araki K, Nagata K. 2011 Functional *in vitro* analysis of the ER01 protein and protein-disulfide isomerase pathway. *J. Biol. Chem.* **286**, 32 705–32 712. (doi:10.1074/jbc.M111.227181)
- Baker KM, Chakravarthi S, Langton KP, Sheppard AM, Lu H, Bulleid NJ. 2008 Low reduction potential of Ero1 $\alpha$  regulatory disulphides ensures tight control of substrate oxidation. *EMBO J.* **27**, 2988–2997. (doi:10.1038/emboj.2008.230)
- Chambers JE, Tavender TJ, Oka OB, Warwood S, Knight D, Bulleid NJ. 2010 The reduction potential of the active site disulfides of human protein disulfide isomerase limits oxidation of the enzyme by Ero1 $\alpha$ . *J. Biol. Chem.* **285**, 29 200–29 207. (doi:10.1074/jbc.M110.156596)
- Masui S, Vavassori S, Fagioli C, Sitia R, Inaba K. 2011 Molecular bases of cyclic and specific disulfide interchange between human ER01 $\alpha$  protein and protein-disulfide isomerase (PDI). *J. Biol. Chem.* **286**, 16 261–16 –271. (doi:10.1074/jbc.M111.231357)
- Gross E, Kastner DB, Kaiser CA, Fass D. 2004 Structure of Ero1p, source of disulfide bonds for oxidative protein folding in the cell. *Cell* **117**, 601–610. (doi:10.1016/S0092-8674(04)00418-0)
- Sevier CS, Kaiser CA. 2006 Disulfide transfer between two conserved cysteine pairs imparts selectivity to protein oxidation by Ero1. *Mol. Biol. Cell* **17**, 2256–2266. (doi:10.1091/mbc.E05-05-0417)
- Kulp MS, Frickel E-M, Ellgaard L, Weissman JS. 2006 Domain architecture of protein-disulfide isomerase facilitates its dual role as an oxidase and an isomerase in Ero1p-mediated disulfide formation. *J. Biol. Chem.* **281**, 876–884. (doi:10.1074/jbc.M511764200)
- Zito E, Chin KT, Blais J, Harding HP, Ron D. 2010 ER01-beta, a pancreas-specific disulfide oxidase, promotes insulin biogenesis and glucose homeostasis. *J. Cell Biol.* **188**, 821–832. (doi:10.1083/jcb.200911086)
- Bulleid NJ, Ellgaard L. 2011 Multiple ways to make disulfides. *Trends Biochem. Sci.* **36**, 485–492. (doi:10.1016/j.tibs.2011.05.004)
- Kakihana T, Nagata K, Sitia R. 2012 Peroxides and peroxidases in the endoplasmic reticulum: integrating redox homeostasis and oxidative folding. *Antioxid. Redox Signal* **16**, 763–771. (doi:10.1089/ars.2011.4238)
- Tavender TJ, Springate JJ, Bulleid NJ. 2011 Recycling of peroxiredoxin IV provides a novel pathway for disulphide formation in the endoplasmic reticulum. *EMBO J.* **29**, 4185–4197. (doi:10.1038/emboj.2010.273)
- Zito E, Melo EP, Yang Y, Wahlander A, Neubert TA, Ron D. 2010 Oxidative protein folding by an endoplasmic reticulum-localized peroxiredoxin. *Mol. Cell.* **40**, 787–797. (doi:10.1016/j.molcel.2010.11.010)
- Nguyen VD *et al.* 2011 Two endoplasmic reticulum PDI peroxidases increase the efficiency of the use of peroxide during disulfide bond formation. *J. Mol. Biol.* **406**, 503–515. (doi:10.1016/j.jmb.2010.12.039)
- Schulman S, Wang B, Li W, Rapoport TA. 2010 Vitamin K epoxide reductase prefers ER membrane-anchored thioredoxin-like redox partners. *Proc. Natl Acad. Sci. USA.* **107**, 15 027–15 032. (doi:10.1073/pnas.1009972107)
- Alon A *et al.* 2012 The dynamic disulphide relay of quiescin sulphhydryl oxidase. *Nature* **488**, 414–418. (doi:10.1038/nature11267)
- Labunskyy VM, Hatfield DL, Gladyshev VN. 2007 The Sep15 protein family: roles in disulfide bond formation and quality control in the endoplasmic reticulum. *IUBMB Life* **59**, 1–5. (doi:10.1080/15216540601126694)
- Chakravarthi S, Jessop CE, Bulleid NJ. 2006 The role of glutathione in disulphide bond formation and endoplasmic-reticulum-generated oxidative stress. *EMBO Rep.* **7**, 271–275. (doi:10.1038/sj.embor.7400645)
- Appenzeller-Herzog C. 2011 Glutathione- and non-glutathione-based oxidant control in the endoplasmic reticulum. *J. Cell Sci.* **124**, 847–855. (doi:10.1242/jcs.080895)
- Benham AM. 2012 The protein disulfide isomerase family: key players in health and disease. *Antioxid. Redox Signal* **16**, 781–789. (doi:10.1089/ars.2011.4439)

41. Vitu E *et al.* 2010 Oxidative activity of yeast Ero1p on protein disulfide isomerase and related oxidoreductases of the endoplasmic reticulum. *J. Biol. Chem.* **285**, 18 155–18 165. (doi:10.1074/jbc.M109.064931)
42. Benham AM, Cabibbo A, Fassio A, Bulleid N, Sitia R, Braakman I. 2000 The CXXCXXC motif determines the folding, structure and stability of human Ero1-L $\alpha$ . *EMBO J.* **19**, 4493–4502. (doi:10.1093/emboj/19.17.4493)
43. Appenzeller-Herzog C, Riemer J, Christensen B, Sorensen ES, Ellgaard L. 2008 A novel disulphide switch mechanism in Ero1 $\alpha$  balances ER oxidation in human cells. *EMBO J.* **27**, 2977–2987. (doi:10.1038/emboj.2008.202)
44. Anelli T *et al.* 2012 Ero1 $\alpha$  regulates Ca<sup>2+</sup> fluxes at the endoplasmic reticulum-mitochondria interface (MAM). *Antioxid. Redox Signal* **16**, 1077–1087. (doi:10.1089/ars.2011.4004)
45. Li G *et al.* 2009 Role of Ero1 $\alpha$ -mediated stimulation of inositol 1,4,5-triphosphate receptor activity in endoplasmic reticulum stress-induced apoptosis. *J. Cell Biol.* **186**, 783–792. (doi:10.1083/jcb.200904060)
46. Gilady SY *et al.* 2010 Ero1 $\alpha$  requires oxidizing and normoxic conditions to localize to the mitochondria-associated membrane (MAM). *Cell Stress Chaperones* **15**, 619–629. (doi:10.1007/s12192-010-0174-1)
47. Lynes EM, Simmen T. 2011 Urban planning of the endoplasmic reticulum (ER): how diverse mechanisms segregate the many functions of the ER. *Biochim. Biophys. Acta* **1813**, 1893–1905. (doi:10.1016/j.bbamcr.2011.06.011)
48. Enyedi B, Varnai P, Geiszt M. 2010 Redox state of the endoplasmic reticulum is controlled by Ero1L- $\alpha$  and intraluminal calcium. *Antioxid. Redox Signal* **13**, 721–729. (doi:10.1089/ars.2009.2880)
49. Li G, Scull C, Ozcan L, Tabas I. 2010 NADPH oxidase links endoplasmic reticulum stress, oxidative stress, and PKR activation to induce apoptosis. *J. Cell Biol.* **191**, 1113–1125. (doi:10.1083/jcb.201006121)
50. Jirapongsananuruk O, Niemela JE, Malech HL, Fleisher TA. 2002 CYBB mutation analysis in X-linked chronic granulomatous disease. *Clin. Immunol.* **104**, 73–76. (doi:10.1006/clim.2002.5230)
51. Anelli T *et al.* 2002 ERp44, a novel endoplasmic reticulum folding assistant of the thioredoxin family. *EMBO J.* **21**, 835–844. (doi:10.1093/emboj/21.4.835)
52. Anelli T *et al.* 2003 Thiol-mediated protein retention in the endoplasmic reticulum: the role of ERp44. *EMBO J.* **22**, 5015–5022. (doi:10.1093/emboj/cdg491)
53. Appenzeller-Herzog C *et al.* 2010 Disulphide production by Ero1 $\alpha$ -PDI relay is rapid and effectively regulated. *EMBO J.* **29**, 3318–3329. (doi:10.1038/emboj.2010.203)
54. Jessop CE, Chakravarthy S, Garbi N, Hammerling GJ, Lovell S, Bulleid NJ. 2007 ERp57 is essential for efficient folding of glycoproteins sharing common structural domains. *EMBO J.* **26**, 28–40. (doi:10.1038/sj.emboj.7601505)
55. Anelli T *et al.* 2007 Sequential steps and checkpoints in the early exocytic compartment during secretory IgM biogenesis. *EMBO J.* **26**, 4177–4188. (doi:10.1038/sj.emboj.7601844)
56. Wang ZV *et al.* 2007 Secretion of the adipocyte-specific secretory protein adiponectin critically depends on thiol-mediated protein retention. *Mol. Cell Biol.* **27**, 3716–3731. (doi:10.1128/MCB.00931-06)
57. Freyaldenhoven S *et al.* 2012 The role of ERp44 in maturation of serotonin transporter protein. *J. Biol. Chem.* **287**, 17 801–17 811. (doi:10.1074/jbc.M112.345058)
58. Cortini M, Sitia R. 2010 From antibodies to adiponectin: role of ERp44 in sizing and timing protein secretion. *Diabetes Obes. Metab.* **12** (Suppl 2), 39–47. (doi:10.1111/j.1463-1326.2010.01272.x)
59. Ronzoni R, Anelli T, Brunati M, Cortini M, Fagioli C, Sitia R. 2010 Pathogenesis of ER storage disorders: modulating Russell body biogenesis by altering proximal and distal quality control. *Traffic* **11**, 947–957. (doi:10.1111/j.1600-0854.2010.01071.x)
60. Higo T, Hattori M, Nakamura T, Natsume T, Michikawa T, Mikoshiba K. 2005 Subtype-specific and ER luminal environment-dependent regulation of inositol 1,4,5-triphosphate receptor type 1 by ERp44. *Cell* **120**, 85–98. (doi:10.1016/j.cell.2004.11.048)
61. Sevier CS, Qu H, Heldman N, Gross E, Fass D, Kaiser CA. 2007 Modulation of cellular disulfide-bond formation and the ER redox environment by feedback regulation of Ero1. *Cell* **129**, 333–344. (doi:10.1016/j.cell.2007.02.039)
62. Heldman N, Vonshak O, Sevier CS, Vitu E, Mehlman T, Fass D. 2010 Steps in reductive activation of the disulfide-generating enzyme Ero1p. *Protein Sci.* **19**, 1863–1876. (doi:10.1002/pro.473)
63. Kim S, Sideris DP, Sevier CS, Kaiser CA. 2012 Balanced Ero1 activation and inactivation establishes ER redox homeostasis. *J. Cell Biol.* **196**, 713–725. (doi:10.1083/jcb.201110090)
64. Inaba K, Masui S, Iida H, Vavassori S, Sitia R, Suzuki M. 2010 Crystal structures of human Ero1 $\alpha$  reveal the mechanisms of regulated and targeted oxidation of PDI. *EMBO J.* **29**, 3330–3343. (doi:10.1038/emboj.2010.222)
65. Wang L, Zhu L, Wang CC. 2011 The endoplasmic reticulum sulfhydryl oxidase Ero1 $\beta$  drives efficient oxidative protein folding with loose regulation. *Biochem. J.* **434**, 113–121. (doi:10.1042/BJ20101357)
66. Dias-Gunasekara S, van Lith M, Williams JAG, Katakly R, Benham AM. 2006 Mutations in the FAD binding domain cause stress-induced misoxidation of the endoplasmic reticulum oxidoreductase Ero1 $\beta$ . *J. Biol. Chem.* **281**, 25 018–25 025. (doi:10.1074/jbc.M602354200)
67. Kosower NS, Kosower EM, Wertheim B, Correa WS. 1969 Diamide, a new reagent for the intracellular oxidation of glutathione to the disulfide. *Biochem. Biophys. Res. Commun.* **37**, 593–596. (doi:10.1016/0006-291X(69)90850-X)
68. Ramming T, Appenzeller-Herzog C. 2012 The physiological functions of mammalian endoplasmic oxidoreductin. I. On disulfides and more. *Antioxid. Redox Signal.* **16**, 1109–1118. (doi:10.1089/ars.2011.4475)
69. Dias-Gunasekara S *et al.* 2005 Tissue specific expression and dimerisation of the endoplasmic reticulum oxidoreductase ero1beta. *J. Biol. Chem.* **280**, 33 066–33 075. (doi:10.1074/jbc.M505023200)
70. Rutkevich LA, Williams DB. 2012 Vitamin K epoxide reductase contributes to protein disulfide formation and redox homeostasis within the endoplasmic reticulum. *Mol. Biol. Cell* **23**, 2017–2027. (doi:10.1091/mbc.E12-02-0102)
71. Gess B, Hofbauer K-H, Wenger RH, Lohaus C, Meyer HE, Kurtz A. 2003 The cellular oxygen tension regulates expression of the endoplasmic oxidoreductase Ero1-L. *Eur. J. Biochem.* **270**, 2228–2235. (doi:10.1046/j.1432-1033.2003.03590.x)
72. May D, Itin A, Gal O, Kalinski H, Feinstein E, Keshet E. 2005 Ero1-L $\alpha$  plays a key role in a HIF-1-mediated pathway to improve disulfide bond formation and VEGF secretion under hypoxia: implication for cancer. *Oncogene* **24**, 1011–1020. (doi:10.1038/sj.onc.1208325)
73. Stockton JD, Merkert MC, Kellaris KV. 2003 A complex of chaperones and disulfide isomerases occludes the cytosolic face of the translocation protein Sec61p and affects translocation of the prion protein. *Biochemistry* **42**, 12 821–12 834. (doi:10.1021/bi035087q)
74. Meunier L, Usherwood YK, Chung KT, Hendershot LM. 2002 A subset of chaperones and folding enzymes form multiprotein complexes in endoplasmic reticulum to bind nascent proteins. *Mol. Biol. Cell* **13**, 4456–4469. (doi:10.1091/mbc.E02-05-0311)
75. Kimata Y, Kohno K. 2011 Endoplasmic reticulum stress-sensing mechanisms in yeast and mammalian cells. *Curr. Opin. Cell Biol.* **23**, 135–142. (doi:10.1016/j.cob.2010.10.008)
76. Hagiwara M *et al.* 2011 Structural basis of an ERAD pathway mediated by the ER-resident protein disulfide reductase ERdj5. *Mol. Cell* **41**, 432–444. (doi:10.1016/j.molcel.2011.01.021)
77. Hagiwara M, Nagata K. 2012 Redox-dependent protein quality control in the endoplasmic reticulum: folding to degradation. *Antioxid. Redox Signal.* **16**, 1119–1128. (doi:10.1089/ars.2011.4495)
78. Chambers JE, Petrova K, Tomba G, Vendruscolo M, Ron D. 2012 ADP ribosylation adapts an ER chaperone response to short-term fluctuations in unfolded protein load. *J. Cell Biol.* **198**, 371–385. (doi:10.1083/jcb.201202005)
79. Jansen G. 2012 An interaction map of ER chaperones and foldases. *Mol. Cell Proteomics* **11**, 710–723. (doi:10.1074/mcp.M111.016550)